THE ASTROPHYSICAL JOURNAL, 562:670–678, 2001 December 1
© 2001. The American Astronomical Society. All rights reserved. Printed in U.S.A.

SN 1998bw/GRB 980425 AND RADIO SUPERNOVAE

KURT W. WEILER
Naval Research Laboratory, Code 7213, Washington, DC 20375-5320; weiler@rsd.nrl.navy.mil
NINO PANAGIA[1]
Space Telescope Science Institute, 3700 San Martin Drive, Baltimore, MD 21218; panagia@stsci.edu
AND
MARCOS J. MONTES
Naval Research Laboratory, Code 7212, Washington, DC 20375-5320; montes@rsd.nrl.navy.mil
Received 2001 April 26; accepted 2001 June 7

ABSTRACT

The unusual supernova SN 1998bw, which is thought to be related to the gamma-ray burster GRB 980425, is a possible link between these two classes of objects. Analyzing the extensive radio emission data available for SN 1998bw, we are able to describe its time evolution within the well-established framework available for the analysis of radio emission from supernovae. This then allows description of a number of physical properties of the object. The radio emission can be best explained as the interaction of a mildly relativistic ($\Gamma \sim 1.6$) shock with a dense, preexplosion stellar wind–established circumstellar medium that is highly structured both azimuthally, in clumps or filaments, and radially, with two observed density enhancements separated by $\sim 3 \times 10^{17}$ cm. With assumptions as to preexplosion stellar wind conditions, it is possible to estimate that the progenitor to SN 1998bw had a mass-loss rate of $\sim 2.6 \times 10^{-5}\ M_{\odot}\ \mathrm{yr}^{-1}$ with at least two $\sim 40\%$ density increases, the most recent extending from ~ 1600 to 4700 yr before explosion and the oldest known having occurred, possibly with comparable length, $\sim 12{,}000$ yr before explosion. Because of its unusual characteristics for a Type Ib/c supernova, the relation of SN 1998bw to GRB 980425 is strengthened, consequently improving our understanding of these poorly understood objects.

Subject headings: gamma rays: bursts — radio continuum: ISM — supernovae: individual (SN 1998bw) — supernova remnants

1. INTRODUCTION

While it is generally accepted that "most" gamma-ray bursters (GRBs) are extremely distant and energetic (see, e.g., Paczynski 1986; Goodman 1986), the discovery of GRB 980425 (Soffitta et al. 1998) on 1998 April 25.90915 and its possible association with the bright supernova SN 1998bw at R.A.(J2000) = $19^{h}35^{m}03\overset{s}{.}31$, decl.(J2000) = $-52°50'44\overset{''}{.}7$ (Tinney et al. 1998) in the relatively nearby spiral galaxy ESO 184-G82 at $z = 0.0085$ (distance ~ 40 Mpc for $H_0 = 65$ km s^{-1} Mpc^{-1}; Galama et al. 1998a, 1998b, 1999; Lidman et al. 1998; Tinney et al. 1998; Sadler et al. 1998; Woosley, Eastman, & Schmidt 1999) has introduced the possibility of a supernova (SN) origin for at least some types of GRBs. The estimated explosion date of SN 1998bw in the interval 1998 April 21–27 (Sadler et al. 1998) corresponds rather well with the time of the GRB 980425 outburst. Iwamoto et al. (1998) feel that they can restrict the core collapse date for SN 1998bw even more from hydrodynamical modeling of exploding C+O stars; and assuming that the SN 1998bw optical light curve is energized by ^{56}Ni decay as in Type Ia SNe, they then place the coincidence between the core collapse of SN 1998bw to within $+0.7/-2$ days of the outburst detection of GRB 980425.

Classified initially as an optical Type Ib SN (Sadler et al. 1998), then Type Ic (Patat & Piemonte 1998), then peculiar Type Ic (Kay, Halpern, & Leighly 1998; Filippenko 1998), then later at an age of 300–400 days as Type Ib again (Patat et al. 1999), SN 1998bw presents a number of optical spectral peculiarities that strengthen the suspicion that it may be the counterpart of the gamma-ray burst.

When the more precise *BeppoSAX* Narrow Field Instruments were pointed at the *BeppoSAX* error box 10 hr after the detection of GRB 980425, two X-ray sources were present (Pian et al. 1999). One of these, named S1 by Pian et al. (1999), was coincident with the position of SN 1998bw and declined slowly between 1998 April and November. The second X-ray source, S2, which was $\sim 4'$ from the position of SN 1998bw, was not detectable again (or at best only marginally with a $< 3\ \sigma$ possible detection 6 days after the initial detection) in follow-up observations in 1998 April, May, and November (Pian et al. 1999, 2000).

However, although a bit of concern remains that the Pian et al. (1999, 2000) X-ray source S2 might have been the brief afterglow from GRB 980425 rather than the Pian source S1 associated with SN 1998bw, Pian et al. (2000) conclude that their source S1 has a "high probability" of being associated with GRB 980425 and that S2 is more likely a variable field source.

In order to analyze the radio emission from SN 1998bw, we shall first collect, rationalize, and extend the formalism that has been so successful in understanding the radio emission from radio supernovae (§ 2) and apply it to SN 1998bw (§ 3). From this we are able to obtain a detailed description of the radio light curves for the object and the physical

[1] Also Astrophysics Division, Space Science Department, European Space Agency.

parameters of the SN system (§ 4). Finally, we compare a number of properties of Type Ib/c SNe and GRBs (§ 5).

2. RADIO SUPERNOVAE

2.1. *Background*

A series of papers published over the past 20 years on radio supernovae (RSNe) has established the radio detection and in a number of cases the radio evolution for approximately two dozen objects: three Type Ib SNe, three Type Ic SNe (N.B.: because the differences between the SN optical classes are slight [Type Ib SNe show strong He I absorption while Type Ic show weak He I absorption] and there are no obvious radio differences, we shall often refer to the classes as Type Ib/c), and the rest Type II SNe. A much larger list of more than 100 additional SNe has low radio upper limits.[2]

In this extensive study of the radio emission from SNe, several effects have been noted: (1) no Type Ia SN has ever been detected at radio wavelengths; (2) Type Ib/c SNe are radio luminous with steep spectral indices (generally $\alpha < -1$; $S \propto \nu^{+\alpha}$) and have a fast turn-on/turnoff, usually peaking at 6 cm near or before optical maximum; and (3) Type II SNe show a range of radio luminosities with flatter spectral indices (generally $\alpha > -1$) and a relatively slow turn-on/turnoff, usually peaking at 6 cm significantly after optical maximum. Type Ib/c may be fairly homogeneous in some of their radio properties while Type II, as in the optical, are quite diverse.

Measurements of the RSN multifrequency radio light curves and their evolution with time show the density and structure of the circumstellar medium (CSM), evidence for possible binary companions, clumpiness or filamentation in the presupernova wind, mass-loss rates and changes therein for the presupernova stellar system, and estimates, through stellar evolution models, of the zero-age main-sequence presupernova stellar mass and the stages through which the star passed on its way to explosion.[3]

2.2. *Radio Supernova Models*

All known RSNe appear to share common properties of (1) nonthermal synchrotron emission with high brightness temperature; (2) a decrease in absorption with time, resulting in a smooth turn-on first at shorter wavelengths and later at longer wavelengths; (3) a power-law decline of the flux density with time at each wavelength after maximum flux density (optical depth ~ 1) is reached at that wavelength; and (4) a final, asymptotic approach of spectral index α ($S \propto \nu^{+\alpha}$) to an optically thin, nonthermal, constant negative value (Weiler et al. 1986; Weiler, Panagia, & Sramek 1990).

Chevalier (1982a, 1982b) has proposed that the relativistic electrons and enhanced magnetic field necessary for synchrotron emission arise from the SN blast wave interacting with a relatively high-density CSM that has been ionized and heated by the initial UV/X-ray flash. This CSM is presumed to have been established by a constant mass-loss ($\dot{M}$) rate and constant velocity ($w_{\rm wind}$) wind [i.e., $\rho \propto \dot{M}/(w_{\rm wind} r^2)$] from a massive stellar progenitor or companion. This ionized CSM is the source of some or all of the initial absorption, although Chevalier (1998) has proposed that synchrotron self-absorption may play a role in some objects.

A rapid rise in the observed radio flux density results from a decrease in these absorption processes as the radio-emitting region expands and the absorption processes, either internal or along the line of sight, decrease. Weiler et al. (1990) have suggested that this CSM can be "clumpy" or "filamentary," leading to a slower radio turn-on; and Montes, Weiler, & Panagia (1997) have proposed at least one example for the presence of a distant ionized medium along the line of sight that is time independent and can cause a spectral turnover at low radio frequencies. In addition to clumps or filaments, the CSM may be structured with significant density irregularities such as rings, disks, shells, or gradients.

2.3. *Radio Supernova Parameterized Radio Light Curves*

Following Weiler et al. (1986, 1990) and Montes et al. (1997) we adopt a parameterized model (the notation is extended and rationalized here from previous publications. However, the "old" notation of τ, τ', and τ'', which has been used previously, is noted where appropriate for continuity):

$$S(\mathrm{mJy}) = K_1\left(\frac{\nu}{5\ \mathrm{GHz}}\right)^{\alpha}\left(\frac{t-t_0}{1\ \mathrm{day}}\right)^{\beta} e^{-\tau_{\rm external}} \times\left(\frac{1-e^{-\tau_{\rm CSM_{clumps}}}}{\tau_{\rm CSM_{clumps}}}\right)\left(\frac{1-e^{-\tau_{\rm internal}}}{\tau_{\rm internal}}\right) \quad (1)$$

with

$$\tau_{\rm external} = \tau_{\rm CSM_{uniform}} + \tau_{\rm distant} = \tau + \tau'' , \quad (2)$$

where

$$\tau_{\rm CSM_{uniform}} = \tau = K_2\left(\frac{\nu}{5\ \mathrm{GHz}}\right)^{-2.1}\left(\frac{t-t_0}{1\ \mathrm{day}}\right)^{\delta} , \quad (3)$$

$$\tau_{\rm distant} = \tau'' = K_4\left(\frac{\nu}{5\ \mathrm{GHz}}\right)^{-2.1} , \quad (4)$$

$$\tau_{\rm CSM_{clumps}} = \tau' = K_3\left(\frac{\nu}{5\ \mathrm{GHz}}\right)^{-2.1}\left(\frac{t-t_0}{1\ \mathrm{day}}\right)^{\delta'} , \quad (5)$$

with K_1, K_2, K_3, and K_4 corresponding, formally, to the flux density (K_1), uniform (K_2, K_4), and clumpy or filamentary (K_3) absorption at 5 GHz 1 day after the explosion date t_0. The terms $\tau_{\rm CSM_{uniform}}$ and $\tau_{\rm CSM_{clumps}}$ describe the attenuation of local uniform CSM and clumpy CSM that are near enough to the SN progenitor that they are altered by its rapidly expanding blast wave. The $\tau_{\rm CSM_{uniform}}$ term is produced by an ionized medium that uniformly covers the emitting source ("uniform external absorption"), and the $(1 - e^{-\tau_{\rm CSM_{clumps}}})\tau^{-1}_{\rm CSM_{clumps}}$ term describes the attenuation produced by an inhomogeneous medium ("clumpy absorption"; see § 2.4 and Natta & Panagia 1984 for a more detailed discussion of attenuation in inhomogeneous media). The $\tau_{\rm distant}$ term describes the attenuation produced by a homogeneous medium that uniformly covers the source but is so far from the SN progenitor that it is not affected by the expanding SN blast wave and is constant in time. All absorbing media are assumed to be purely thermal, singly ionized gases that absorb via free-free transitions with frequency dependence $\nu^{-2.1}$ in the radio. The parameters δ and δ' describe the time dependence of the

[2] These can be found at http://rsd-www.nrl.navy.mil/7214/weiler/kwdata/RSNtable.txt.

[3] A summary of the radio information on SNe can be found at http://rsd-www.nrl.navy.mil/7214/weiler/sne-home.html.

optical depths for the local uniform and clumpy or filamentary media, respectively.

The free-free optical depth outside the emitting region is proportional to the integral of the square of the CSM density over the radius. Since in the simple Chevalier model the CSM density decreases as r^{-2}, the external optical depth will be proportional to r^{-3}; and since the radius increases as a power of time, $r \propto t^m$ with $m \leq 1$ (i.e., $m = 1$ for undecelerated blast-wave expansion), it follows that the deceleration parameter m is

$$m = \frac{-\delta}{3} . \tag{6}$$

The model by Chevalier (1982a, 1982b) relates β and δ to the energy spectrum of the relativistic particles γ ($\gamma = 2\alpha - 1$) by $\delta = \alpha - \beta - 3$ so that for cases where $K_2 = 0$ and δ is therefore indeterminate, we can use

$$m = -\frac{\alpha - \beta - 3}{3} . \tag{7}$$

Since it is physically realistic and may be needed in some RSNe where radio observations have been obtained at early times and high frequencies, we have also included in equation (1) the possibility for an internal absorption term.[4] This internal absorption term ($\tau_{\rm internal}$) may consist of two parts: synchrotron self-absorption (SSA; $\tau_{\rm internal_{SSA}}$) and mixed, thermal free-free absorption/nonthermal emission ($\tau_{\rm internal_{ff}}$):

$$\tau_{\rm internal} = \tau_{\rm internal_{SSA}} + \tau_{\rm internal_{ff}} , \tag{8}$$

$$\tau_{\rm internal_{SSA}} = K_5 \left(\frac{\nu}{5\ {\rm GHz}}\right)^{\alpha - 2.5} \left(\frac{t - t_0}{1\ {\rm day}}\right)^{\delta''} , \tag{9}$$

$$\tau_{\rm internal_{ff}} = K_6 \left(\frac{\nu}{5\ {\rm GHz}}\right)^{-2.1} \left(\frac{t - t_0}{1\ {\rm day}}\right)^{\delta'''} , \tag{10}$$

with K_5 corresponding, formally, to the internal nonthermal ($\nu^{\alpha - 2.5}$) SSA and K_6 corresponding, formally, to the internal thermal ($\nu^{-2.1}$) free-free absorption mixed with nonthermal emission, at 5 GHz 1 day after the explosion date t_0. The parameters δ'' and δ''' describe the time dependence of the optical depths for the SSA and free-free internal absorption components, respectively.

A cartoon of the expected structure of an SN and its surrounding media is presented in Figure 1 (see also Lozinskaya 1992). The radio emission is expected to arise near the blast wave (Chevalier & Fransson 1994).

2.4. *Radio Supernova Results*

The success of the basic parameterization and model has been shown in the relatively good correspondence between the model fits and the data for all subtypes of RSNe, e.g., Type Ib SN 1983N (Sramek, Panagia, & Weiler 1984), Type Ic SN 1990B (Van Dyk et al. 1993a), Type II SN 1979C (Weiler et al. 1991, 1992b; Montes et al. 2000) and SN 1980K (Weiler et al. 1992a; Montes et al. 1998), and Type IIn SN 1988Z (Van Dyk et al. 1993b; Williams et al. 2002). Note that after day $\sim$4000, the evolution of the radio emission from both SN 1979C and SN 1980K deviates from the expected model evolution and that SN 1979C shows a sinusoidal modulation in its flux density prior to day $\sim$4000. A more detailed discussion of radio observations of SNe and of modeling results is given in Weiler et al. (2001)

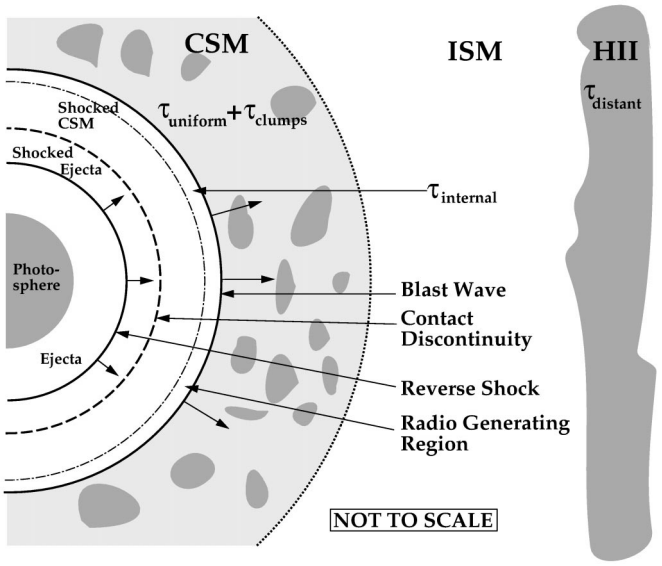


FIG. 1.—Cartoon, not to scale, of the SN and its shocks, along with the stellar wind–established CSM and more distant ionized material. Radio emission is thought to arise near the blast wave. Expected locations of the several absorbing terms in eqs. (1)–(10) are illustrated.

Thus, the radio emission from SNe appears to be relatively well understood in terms of blast-wave interaction with a structured CSM, as described by the Chevalier (1982a, 1982b) model and its extensions by Weiler et al. (1986, 1990) and Montes et al. (1997). For instance, the fact that the uniform external absorption exponent δ is about -3, or somewhat less, for most RSNe is evidence that the absorbing medium is generally a $\rho \propto r^{-2}$ wind, as expected from a massive stellar progenitor that explodes in the red supergiant phase. Additionally, in their study of the radio emission from SN 1986J, Weiler et al. (1990) found that the simple Chevalier (1982a, 1982b) model could not describe the relatively slow turn-on. They therefore included terms described mathematically by $\tau_{\rm CSM_{clumps}}$ in equations (1) and (5). This extension greatly improved the quality of the fit and was interpreted by Weiler et al. (1990) to represent the possible presence of filaments or clumps in the CSM. Such a clumpiness in the wind material was again required for modeling the radio data from SN 1988Z (Van Dyk et al 1993a) and SN 1993J (Van Dyk et al. 1994). Since that time, evidence for filamentation in the envelopes of SNe has also been found from optical and UV observations (e.g., Filippenko, Matheson, & Barth 1994; Spyromilio 1994).

From this modeling, there are a number of physical properties of SNe that we can determine from radio observations.

2.4.1. *Mass-Loss Rate from Radio Absorption*

From the Chevalier (1982a, 1982b) model, the turn-on of the radio emission for RSNe provides a measure of the

[4] Note that for simplicity we use an internal absorber attenuation of the form $(1 - e^{-\tau_{\rm CSM_{internal}}})/\tau_{\rm CSM_{internal}}$, which is appropriate for a plane-parallel geometry, instead of the more complicated expression (e.g., Osterbrock 1974) valid for the spherical case. The assumption does not affect the quality of our analysis because, to within 5% accuracy, the optical depth obtained with the spherical case formula is simply three-fourths of that obtained with the plane-parallel slab formula.

presupernova mass-loss rate/wind velocity ratio ($\dot{M}/w_{\rm wind}$). Weiler et al. (1986) derived this ratio for the case of pure, external absorption by a uniform medium. However, we now recognize that there are several possible origins for absorption and generalize equation (16) of Weiler et al. (1986) to

$$\frac{\dot{M}(M_\odot\ \mathrm{yr}^{-1})}{(w_{\rm wind}/10\ \mathrm{km\ s}^{-1})} = (3.0\times10^{-6})\langle\tau_{\rm eff}^{0.5}\rangle m^{-1.5} \times\left(\frac{v_i}{10^4\ \mathrm{km\ s}^{-1}}\right)^{1.5}\left(\frac{t_i}{45\ \mathrm{days}}\right)^{1.5} \times\left(\frac{t}{t_i}\right)^{1.5m}\left(\frac{T}{10^4\ \mathrm{K}}\right)^{0.68}. \quad (11)$$

Since the appearance of optical lines for measuring SN ejecta velocities is often delayed a bit relative to the time of the explosion, we arbitrarily take $t_i = 45$ days. Because our observations have shown that generally $0.8 \le m \le 1.0$ and from equation (11) that $\dot{M} \propto t_i^{1.5(1-m)}$, the dependence of the calculated mass-loss rate on the date t_i of the initial ejecta velocity measurement is weak: $\dot{M} \propto t_i^{<0.3}$. Thus, we can take the best optical or VLBI velocity measurements available without worrying about the deviation of their exact measurement epoch from the assumed 45 days after explosion. For convenience, and because many SN measurements indicate velocities of $\sim$10,000 km s^{-1}, we take $v_i = v_{\rm blastwave} = 10{,}000$ km s^{-1}. We also normally adopt values of $T = 20{,}000$ K, $w_{\rm wind} = 10$ km s^{-1} (which is appropriate for a red supergiant wind), $t = (t_{6\rm cmpeak} - t_0)$ days from our best fits to the radio data for each RSN, and m from equation (6) or (7), as appropriate. The optical depth term $\langle\tau_{\rm eff}^{0.5}\rangle$, however, is not as simple as that used by Weiler et al. (1986).

We are now able to identify at least three possible absorption regimes: (1) absorption by a uniform external medium, (2) absorption by a clumpy or filamentary external medium with a statistically large number of clumps, and (3) absorption by a clumpy or filamentary medium with a statistically small number of clumps. These three cases have different formulations for $\langle\tau_{\rm eff}^{0.5}\rangle$.

2.4.1.1. Absorption by a Uniform External Medium

This is the simplest case and has been treated by Weiler et al. (1986). Their result is obtained by substituting

$$\langle\tau_{\rm eff}^{0.5}\rangle = \tau_{\rm CSM_{uniform}}^{0.5} \quad (12)$$

which is the uniform absorption described in equation (3).

2.4.1.2. Absorption by a Statistically Large Number of Clumps or Filaments

If the number density and the geometric cross section of clumps is large enough so that any line of sight from the emitting region intersects many clumps, then we can use a statistical approach in a scenario that sees numerous clumps immersed in a uniform medium. For the case of $\delta = \delta'$, it is clear that the fraction of clumpy material remains constant throughout the whole wind-established CSM, and therefore, the radio signal from the SN suffers an absorption $\tau_{\rm CSM_{uniform}}$ from the uniform component of the CSM plus an additional absorption, with an even probability distribution between 0 and $\tau_{\rm CSM_{clumps}}$, from the clumpy or filamentary component of the CSM. In such a case the appropriate average over the possible extremes of the optical depth is defined as

$$\langle\tau_{\rm eff}^{0.5}\rangle = 0.67[(\tau_{\rm CSM_{uniform}} + \tau_{\rm CSM_{clumps}})^{1.5} - \tau_{\rm CSM_{uniform}}^{1.5}]\tau_{\rm CSM_{clumps}}^{-1} \quad (13)$$

with $\tau_{\rm CSM_{uniform}}$ and $\tau_{\rm CSM_{clumps}}$ described in equations (3) and (5). Note that in the limit of $\tau_{\rm CSM_{clumps}} \to 0$ then $\langle\tau_{\rm eff}^{0.5}\rangle \to \tau_{\rm CSM_{uniform}}$ and in the limit of $\tau_{\rm CSM_{uniform}} \to 0$ then $\langle\tau_{\rm eff}^{0.5}\rangle \to 0.67\tau_{\rm CSM_{clumps}}$.

2.4.1.3. Absorption by a Statistically Small Number of Clumps or Filaments

When the number density is small and the probability that the line of sight from a given clump intersects another clump is low, then both the emission and the absorption will occur effectively within each clump. We still expect a situation with a range of optical depths from zero for clumps on the far side of the blast wave–CSM interaction region to a maximum corresponding to the optical depth through a clump for clumps on the near side of the blast wave–CSM interaction region. We also expect an attenuation of the form $(1 - e^{-\tau_{CSM_{\rm clumps}}})\tau_{\rm CSM_{clumps}}^{-1}$ but now $\tau_{\rm CSM_{clumps}}$ represents the optical depth along a clump diameter. Moreover, in this case the clumps occupy only a small fraction of the volume and have a volume filling factor of $\phi \ll 1$. Since the probability that the line of sight from a given clump intersects another clump is low, a condition between the size of a clump, the number density of clumps, and the radial coordinate can be written as

$$\eta\pi r^2 R \approx N < 1 \quad (14)$$

where η is the volume number density of clumps, r is the radius of a clump, R is the distance from the center of the SN to the blast wave–CSM interaction region, and N is the average number of clumps along the line of sight with N appreciably lower than unity by definition. It is easy to verify that there is a relation between the volume filling factor ϕ, r, R, and N, of the form

$$\phi = \frac{4}{3}\frac{r}{R}N\ . \quad (15)$$

We now find that we can express the effective optical depth $\langle\tau_{\rm eff}^{0.5}\rangle$ as

$$\langle\tau_{\rm eff}^{0.5}\rangle = 0.47\tau_{\rm CSM_{clumps}}^{0.5}\phi^{0.5}N^{0.5}\ , \quad (16)$$

where for initial estimates, we shall generally take $N \sim 0.5$ and a constant ratio $rR^{-1} \sim 0.33$ so that, from equation (15), $\phi \sim 0.22$.

While intermediate cases between these three will yield results with larger errors, it is felt, considering other uncertainties in the assumptions, that equation (11) with the relations for $\langle\tau_{\rm eff}^{0.5}\rangle$ given in equations (12), (13), and (16) yield reasonable estimates of the mass-loss rates of the presupernova star. Mass-loss rate estimates from radio absorption obtained in this manner tend to be $\sim10^{-6}\ M_\odot$ yr^{-1} for Type Ib/c SNe and $\sim10^{-4}$–$10^{-5}\ M_\odot$ yr^{-1} for Type II SNe.

2.4.2. *Mass-Loss Rate from Radio Emission*

For comparison purposes, we can also try to estimate the presupernova mass-loss rate that established the CSM by considering the radio emission directly. From the Chevalier model and Weiler et al. (1989), one can write the radio

emission from an RSN in the following form:

$$\frac{\dot{M}(M_\odot\ \mathrm{yr}^{-1})}{(w_{\mathrm{wind}}/10\ \mathrm{km\ s}^{-1})} = 8.6 \times 10^{-9} \times \left(\frac{L_{6\ \mathrm{cm\ peak}}}{10^{26}\ \mathrm{ergs\ s}^{-1}\ \mathrm{Hz}^{-1}}\right)^{0.71} \times \left[\frac{t_{6\ \mathrm{cm\ peak}} - t_0}{(\mathrm{days})}\right]^{1.14} \quad (17)$$

for Type Ib/c SNe, and

$$\frac{\dot{M}(M_\odot\ \mathrm{yr}^{-1})}{(w_{\mathrm{wind}}/10\ \mathrm{km\ s}^{-1})} = 1.0 \times 10^{-6} \times \left(\frac{L_{6\ \mathrm{cm\ peak}}}{10^{26}\ \mathrm{ergs\ s}^{-1}\ \mathrm{Hz}^{-1}}\right)^{0.54} \times \left[\frac{t_{6\ \mathrm{cm\ peak}} - t_0}{(\mathrm{days})}\right]^{0.38} \quad (18)$$

for Type II SNe, assuming an absorption of $\tau_{6\mathrm{cmpeak}} \sim 1$, from whatever origin, at the time of observed peak in the 6 cm flux density.

The coefficients in equations (17) and (18) depend on the amount of kinetic energy that is transferred to accelerate relativistic electrons and on the details of the acceleration mechanism. Although Fermi acceleration is generally accepted as the relativistic electron acceleration process and it is usually assumed that some fixed fraction of the explosion kinetic energy is transformed into relativistic synchrotron electrons (often assumed $\sim$1%), the physics of these two aspects is not known in detail a priori. Therefore, equations (17) and (18) can only be "calibrated" by using the values of well-studied RSNe and the assumption that all RSNe of the same type will have similar characteristics. The constants in equations (17) and (18) have thus been determined from averages within the two RSN subtypes (Type Ib/c and Type II) of those RSNe that have pure, uniform absorption (i.e., $K_3 = 0$), with the omission of SN 1987A because of its blue rather than red supergiant progenitor.

It should be kept in mind that because the detailed mechanism of radio emission from SNe is not well understood and the estimates have to rely on ad hoc calibrations from the few RSNe that have well-measured light curves, mass-loss rates estimated from equations (17) and (18) can only complement, and perhaps support, the more accurate determinations made from radio absorption.

2.4.3. *Changes in Mass-Loss Rate*

A particularly interesting case of mass loss from an RSN is SN 1993J, where detailed radio observations are available starting only a few days after explosion. Van Dyk et al. (1994) find evidence for a *changing* mass-loss rate for the presupernova star that was as high as $\sim 10^{-4}\ M_\odot\ \mathrm{yr}^{-1}$ approximately 1000 yr before explosion and decreased to $\sim 10^{-5}\ M_\odot\ \mathrm{yr}^{-1}$ just before explosion, resulting in a relatively flat density profile of $\rho \propto r^{-1.5}$.

Fransson & Björgsson (1998) have suggested that the observed behavior of the free-free absorption for SN 1993J could alternatively be explained in terms of a systematic decrease of the electron temperature in the circumstellar material as the SN expands. It is not clear, however, what the physical process is that determines why such a cooling might occur efficiently in SN 1993J but not in SNe such as SN 1979C and SN 1980K, where no such behavior is required to explain the observed radio turn-on characteristics. Also, recent X-ray observations of SN 1993J with *ROSAT* imply a non-r^{-2} CSM density surrounding the SN progenitor (Immler, Aschenbach, & Wang 2001), with a density gradient of $\rho \propto r^{-1.6}$.

Moreover, changes in presupernova mass-loss rates are not unusual. Montes et al. (2000) find that Type II SN 1979C had a slow increase in its radio light curve after day $\sim$4300, which implies an *excess* in flux density by a factor of $\sim$1.7 with respect to the standard model, or a density enhancement of $\sim$30% over the expected density at that radius. On the other hand, Type II SN 1980K showed a steep *decline* in flux density at all wavelengths by a factor of $\sim$2 occurring between days $\sim$3700 and $\sim$4900. Such a sharp decline in flux density implies a *decrease* in ρ_{CSM} by a factor of $\sim$1.6 below that expected for a r^{-2} CSM density profile (Montes et al. 1998). If one assumes that the radio emission arises from a $\sim 10^4$ km s^{-1} blast wave traveling through a CSM established by a $\sim$10 km s^{-1} preexplosion stellar wind, this implies a significant change in the stellar mass-loss rate for a constant speed wind at $\sim$12,000 yr before explosion for both SNe.

3. SN 1998bw

The radio emission from SN 1998bw reached an unusually high 6 cm spectral luminosity at a peak of $\sim 6.7 \times 10^{28}$ ergs s^{-1} Hz^{-1}, i.e., $\sim$3 times higher than either of the well-studied, very radio luminous Type IIn SN 1986J and SN 1988Z, and $\sim$40 times higher than the average peak 6 cm spectral luminosity of Type Ib/c SNe. It also reached this 6 cm peak rather quickly, only $\sim$13 days after explosion.

SN 1998bw is unusual in its radio emission but is not extreme. For example, the times from explosion to peak 6 cm luminosity for both SN 1987A and SN 1983N were shorter, and in spite of the fact that SN 1998bw has been called "the most luminous RSN ever observed," its 6 cm spectral luminosity at peak is exceeded by that of SN 1982aa (Yin 1994). However, SN 1998bw is certainly the most radio-luminous Type Ib/c RSN observed so far by a factor of $\sim$25, and it reached this higher radio luminosity very early.

3.1. *Expansion Velocity*

Although unique in neither the speed of radio light-curve evolution nor in peak 6 cm radio luminosity, SN 1998bw is certainly unusual in the combination of these two factors: it is very radio luminous very soon after explosion. Kulkarni et al. (1998a, 1998b) have used these observed qualities, together with the lack of interstellar scintillation at early times, brightness temperature estimates, and physical arguments, to conclude that the blast wave from SN 1998bw that gives rise to the radio emission must have been expanding relativistically. On the other hand, Waxman & Loeb (1999) argue that a subrelativistic blast wave can generate the observed radio emission. However, both sets of authors agree that a very high expansion velocity ($\gtrsim 0.3c$) is required for the radio-emitting region under a spherical geometry.

Simple arguments confirm this high velocity. To avoid the well-known Compton catastrophe, Kellermann & Pauliny-Toth (1969) have shown that the brightness temperature $T_B < 10^{12}$ K must hold, and Readhead (1994) has better defined this limit to $T_B < 10^{11.5}$ K. From geometrical arguments, such a limit requires the radiosphere of SN 1998bw to have expanded at an apparent speed of $\gtrsim 230{,}000$ km s^{-1} at least during the first few days after explosion. While such a value is only mildly relativistic ($\Gamma \sim 1.6$; $\Gamma = 1/[1 - (v^2/c^2)]^{1/2}$), it is still unusually high. Measurements by Gaensler et al. (1997) and Manchester (2001) have demonstrated that the radio-emitting regions of the Type II SN 1987A expanded at an *average* velocity of $\sim 35{,}000$ km s^{-1} over the 3 yr from 1987 February to mid-1990, so in a very low density environment, such as one finds around Type Ib/c SNe, very high blast-wave velocities appear to be possible.

3.2. *Radio Light Curves*

An obvious comparison of SN 1998bw with other RSNe is the evolution of its radio flux density at multiple frequencies and its description by known RSN models. The available radio data[5] are plotted in Figure 2. SN 1998bw shows an early peak that reaches a maximum as early as days 10–12 at 8.64 GHz, a minimum almost simultaneously for the higher frequencies ($\nu \geq 2.5$ GHz) at days $\sim$20–24, then a secondary, somewhat lower, peak at later times after the first dip. An interesting characteristic of this "double-humped" structure is that it dies out at lower frequencies and is relatively inconspicuous in the 1.38 GHz radio measurements (see Fig. 2).

Li & Chevalier (1999) propose an initially synchrotron self-absorbed, rapidly expanding blast wave in a $\rho \propto r^{-2}$ circumstellar wind model to describe the radio light curve for SN 1998bw. This is in many ways similar to the Chevalier (1998) model for Type Ib/c SNe, which also included SSA. To produce the second peak in the radio light curves, Li & Chevalier (1999) postulate a boost of blast-wave energy by a factor of $\sim$2.8 on day $\sim$22 in the observer's time frame.

Modeling of the radio data for SN 1998bw with the well-established formalism for RSNe presented above shows that such an energy boost is not needed. A fast shock interacting with a dense, slow, stellar wind–established ionized CSM that is modulated in density over timescales similar to those seen for RSNe can produce a superior fit to the data. No blast-wave reacceleration is required, and no SSA at early times is apparent. The parameters of our best-fit model are given in Table 1 and shown as the curves in Figure 2. Li & Chevalier (1999) do not give a quantitative indication of the quality of their fit. However, a visual comparison of the curves in Figure 2 with those of Li & Chevalier's (1999)

[5] Radio data are available at http://www.narrabri.atnf.csiro.au/mwiering/grb/grb980425/.

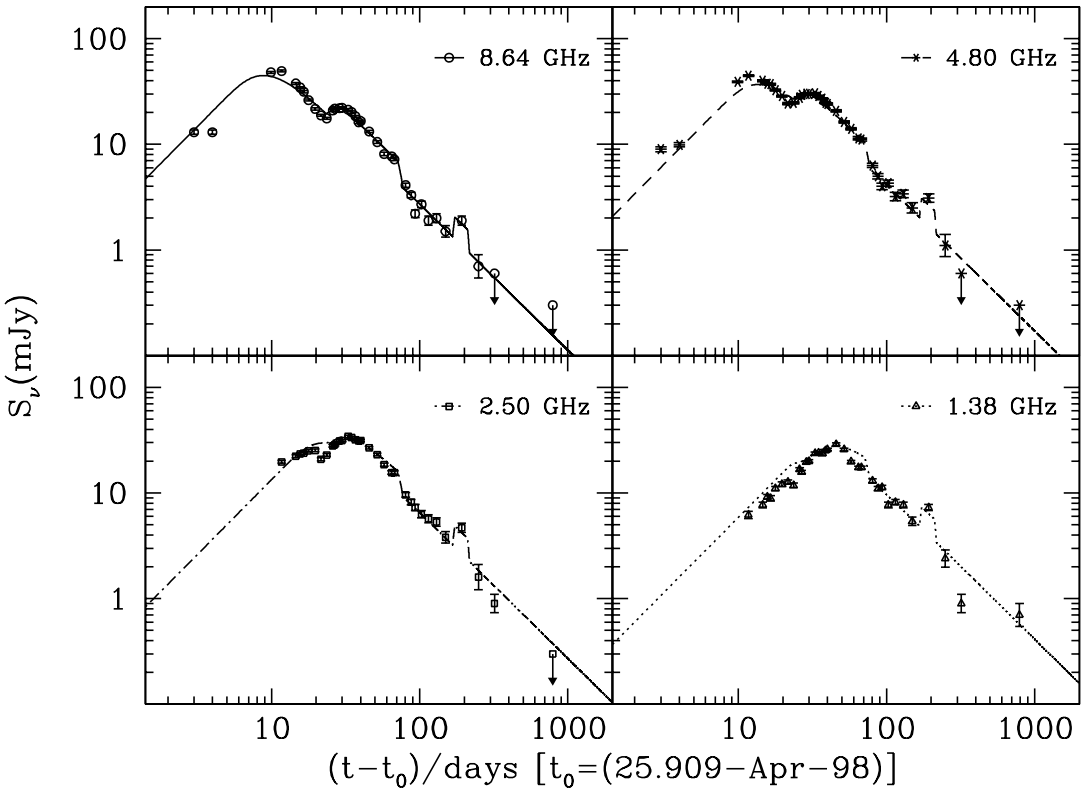


FIG. 2.—Radio light curves of SN 1998bw at 8.64 GHz (3.5 cm; *upper left*: *open circles*, *solid line*), 4.80 GHz (6.3 cm; *upper right*: *stars*, *dashed line*), 2.50 GHz (12 cm; *lower left*: *open squares*, *dash-dotted line*), and 1.38 GHz (21.7 cm; *lower right*: *open triangles*, *dotted line*). Curves are derived from a best-fit model described by the eqs. (1)–(10) and the parameters and assumptions listed in Table 1. During the 50 day intervals from days 25–75 and 165–215, the emission and absorption terms (K_1 and K_3) are increased by factors of 1.6 and 2.0, respectively, corresponding to a density increase of 40%, with a 6 day boxcar smoothed turn-on and turnoff of the enhanced emission/absorption. The physical interpretation of these enhancements is discussed in § 4.

TABLE 1

SN 1998bw Modeling Results

Parameter	Value
α	-0.71
β	-1.38
K_1[a]	2.4×10^3
K_2	0
δ	...
K_3[a]	1.7×10^3
δ'	-2.80
K_4	1.2×10^{-2}
t_0 (explosion date)	1998 Apr. 25.90915
$t_{6\ \mathrm{cm\ peak}} - t_0$ (days)	13.3
$S_{6\ \mathrm{cm\ peak}}$ (mJy)	37.4
d (Mpc)	38.9
$L_{6\ \mathrm{cm\ peak}}$ (ergs s^{-1} Hz^{-1})	6.7×10^{28}
$\dot{M}$ ($M_\odot$ yr^{-1})[b]	2.6×10^{-5}

[a] Enhanced by factors of 1.6 (K_1) and 2.0 (K_3), corresponding to a density increase of 40%, over the intervals of days 25–75 and days 165–215, although the latter interval could be as long as 100 days and still be compatible with the available data.

[b] Assuming $t_i = 23$ days, $t = (t_{6\ \mathrm{cm\ peak}} - t_0) = 13.3$ days, $m = -(\alpha - \beta - 3)/3 = 0.78$, $w_{\mathrm{wind}} = 10$ km s^{-1}, $v_i = v_{\mathrm{blast\ wave}} = 230{,}000$ km s^{-1}, $T = 20{,}000$ K, average number of clumps along the line of sight $N = 0.5$ and volume filling factor $\phi = 0.22$.

Figure 9 shows that our purely thermal absorption model with structured CSM provides a superior fit.

4. DISCUSSION

4.1. *Radio Light-Curve Description*

An unusual feature of the SN 1998bw radio light curves shown in Figure 2 is its apparently "double-humped" structure, with a second peak in the radio emission near day $\sim$30. Such a double-humped structure of the radio light curves can be reproduced by a single energy blast wave encountering differing CSM density regimes as it travels rapidly outward. This is a reasonable assumption since complex density structure in the CSM surrounding SNe, giving rise to structure in the radio light curves, is very well known in such objects as SN 1979C (Weiler et al. 1991, 1992b; Montes et al. 2000), SN 1980K (Weiler et al. 1992a; Montes et al. 1998), SN 1988Z (Van Dyk et al. 1993b; Williams et al. 2002), and particularly SN 1987A (Jakobsen et al. 1991).

Additionally, what has not been previously recognized is a sharp drop in the radio emission near day $\sim$75 and a single measurement epoch at day 192, which is significantly ($\sim$60%) higher at all frequencies than expected from the preceding data on day 149 and the following data on day 249.

Quite surprisingly, both of these temporary increases in radio emission can be explained by the SN blast wave encountering physically similar shells of enhanced density. The first enhancement or "bump" after the initial outburst peak is estimated to start on day 25 and end on day 75; i.e., it has a duration of $\sim$50 days and turn-on and turnoff times of about 12 days, where the increased radio emission (K_1) by a factor of 1.6 and absorption (K_3) by a factor of 2.0 imply a density enhancement of $\sim$40% for no change in clump size. Exactly the same density enhancement factor and length of enhancement are compatible with the "bump" observed in the radio emission at day 192 (i.e., the single measurement within the 100 day gap between measurements on days 149 and 249), even though the logarithmic timescale of Figure 2 makes the time interval look much shorter. Unfortunately, the decreased sampling interval has only one set of measurements altered by the proposed day 192 enhancement, so we cannot determine its length other than that it is less than 100 days.

Note that the fit listed in Table 1 and shown as the curves in Figure 2 requires no "uniform" absorption ($K_2 = 0$) so that all of the free-free absorption is due to a clumpy medium, as described in equations (1) and (5). These results, combined with the estimate of a high blast-wave velocity, suggest that the CSM around SN 1998bw is highly structured with little, if any, interclump gas. The clump filling factor has to be high enough to intercept a considerable fraction of the blast-wave energy and low enough to let radiation escape from any given clump without being appreciably absorbed by any other clump (see 2.4.1 case 3). The blast wave can then easily move at a speed that is a significant fraction of the speed of light because it is moving in a very low-density medium but still cause strong energy dissipation and relativistic electron acceleration at the clump surfaces facing the SN explosion center.

Note also from the fit given in Table 1 that the presence of a K_4 factor implies that there is a more distant, uniform screen of ionized gas surrounding the exploding system, which is too far to be affected by the rapidly expanding blast wave and provides a time-independent absorption.

4.2. *Physical Parameter Estimates*

Using the fitting parameters from Table 1 and equations (11) and (16), we can estimate a mass-loss rate from the preexplosion star. However, the proper parameter assumptions are rather uncertain for these enigmatic objects. For a preliminary estimate we shall assume $t_i = 23$ days, $t = (t_{6\ \mathrm{cm\ peak}} - t_0) = 13.3$ days, $m = -(\alpha - \beta - 3)/3 = 0.78$ (eq. [7]), $w_{\mathrm{wind}} = 10$ km s^{-1} (for an assumed red supergiant progenitor), $v_i = v_{\mathrm{blastwave}} = 230{,}000$ km s^{-1}, and $T = 20{,}000$ K. We shall also assume, since the radio emission implies that the CSM is highly clumped (i.e., $K_2 = 0$), that the CSM volume is only sparsely occupied ($N = 0.5$, $\phi = 0.22$). Within these rather uncertain assumptions, equations (11) and (16) yield an estimated mass-loss rate of $\dot{M} \sim 2.6 \times 10^{-5}\ M_\odot$ yr^{-1}, with density enhancements of $\sim$40%, during the two known extended "bump" periods.

Assuming that the blast wave is traveling at a constant speed of $\sim$230,000 km s^{-1}, the start of the first "bump" on day 25 implies that it starts at $\sim 5.0 \times 10^{16}$ cm, and it ends on day 75 at $\sim 1.5 \times 10^{17}$ cm from the star. Correspondingly, if it was established by a 10 km s^{-1} red supergiant wind, the 50 days of enhanced mass loss started $\sim$4,700 yr and ended $\sim$1,600 yr before the explosion. The earlier high mass-loss rate epoch indicated by the enhanced emission on day 192 in the measurement gap between day 149 and day 249 implies, with the same assumptions, that it occurred in the interval between $\sim$9,400 and $\sim$15,700 yr before explosion. It is interesting to note that the time between the presumed centers of the first and second increased mass-loss episodes of $\sim$9,400 yr is comparable to the $\sim$12,000 yr before explosion at which SN 1979C had a significant mass-loss rate increase (Montes et al. 2000) and SN 1980K had a significant mass-loss rate decrease (Montes et al. 1998), thus

establishing a possible characteristic timescale of $\sim 10^4$ yr for significant changes in mass-loss rate for preexplosion massive stars. As discussed by Panagia & Bono (2001) and G. Bono & N. Panagia (2002, in preparation), mass-loss variations with such timescales can be explained in terms of pulsational instabilities of red supergiants with initial masses of $\sim 20\ M_\odot$.

5. GRB RADIO AFTERGLOWS AND TYPE Ib/c RADIO SUPERNOVAE

Since the suggestion of a possible relation between SN 1998bw and GRB 980425, it has remained a tantalizing possibility that the origin of at least some GRBs is in the better known Type Ib/c SN phenomenon. First, of course, one must keep in mind that there may be (and probably is) more than one origin for GRBs, a situation which is true for most other classes of objects. For example, SNe, after having been identified as a new phenomenon in the early part of the last century, quickly split into several subgroups, such as Zwicky's Types I–VI, then coalesced back into just two subgroupings based on whether Hα was absent (Type I) or present (Type II) in their optical spectra. This simplification has not withstood the test of time, however, and subgroupings of Types Ia, Ib, Ic, II, IIb, IIpec, IIn, and others have come into use over the past 20 years.

GRBs, although at a much earlier stage of understanding, have similarly started to split into subgroupings. The two currently accepted groupings are referred to as "fast hard" and "slow soft," from the tendency of the gamma-ray emission for some to evolve more rapidly (mean duration ~ 0.2 s) and have a somewhat harder spectrum than for others that evolve more slowly (mean duration ~ 20 s) with a somewhat softer spectrum (Fishman & Meegan 1995).

Since we are only concerned with the radio afterglows of GRBs here, all of our examples fall into the "slow soft" classification, at least partly because the "fast hard" GRBs fade too quickly for follow-up observations to obtain the precise positional information needed for identification at longer wavelengths. It is therefore uncertain at present whether "fast hard" GRBs have radio afterglows or even whether the "slow soft" GRBs represent a single phenomenon. If, however, we assume that all "slow soft" GRBs have a similar origin and that GRB 980425/SN 1998bw is a key to this puzzle telling us that "slow-soft" GRBs have their origin in Type Ib/c SNe, we can investigate relations between the two observational phenomena.

Keeping in mind that much of the radio data available on Type Ib/c SNe is of poor quality owing to their relative faintness and that the situation is even worse for GRB radio afterglows, some of the similarities are as follows:

1. GRB 980425 and Type Ib SN 1998bw are possibly related.
2. Both GRBs and Type Ib/c SNe are suggested by some models to originate from the core collapse of a massive (perhaps stripped) progenitor star.
3. Both GRBs and Type Ib/c SNe are suggested by some models to release $\sim 10^{51}$–10^{52} ergs of kinetic energy in a few seconds.
4. Both GRBs and Type Ib/c SNe are detectable at centimeter wavelengths very soon (within a few days) after the explosion while Type II SNe generally have much longer delays.
5. Both GRBs and Type Ib/c RSNe generally have relatively steep radio spectra ($\alpha \lesssim -1$; $S \propto \nu^{+\alpha}$) compared to, e.g., extragalactic quasi-stellar objects, radio galaxy nuclei ($\alpha \gtrsim -0.75$), or Type II RSNe ($\alpha \gtrsim -1$).

There is presently one clear difference between known GRBs and Type Ib/c SNe, however. Type Ib/c RSNe can generally be treated as classical nonrelativistic phenomena, sufficiently close that cosmological effects can be neglected, while most known GRBs appear to be highly relativistic phenomena ($\Gamma \sim 10$) at cosmological distances ($z \sim 1$). SN 1998bw/GRB 980425, which is not very distant ($z = 0.0085$, ~ 40 Mpc) and is only mildly relativistic ($\Gamma \sim 1.6$), is possibly the "bridge" between the two groups. We shall discuss the properties of specific GRBs in more detail in a following paper.

While observational similarity does not necessarily mean identical physical processes, the possibility of similar or related phenomena giving rise to both GRBs and Type Ib/c SNe must be considered. Speculatively, GRBs may represent a rare subclass of Type Ib/c SNe and/or the subset of Type Ib/c SNe, where we lie within the narrow emission cone of a relativistic jet. In either case, they are sufficiently rare that they can be found only by sampling very large volumes of space, i.e., preferentially at high redshifts.

6. SUMMARY

We have collected and rationalized a parameterization and physical model description that has been very successful in explaining the radio emission from SNe. We have applied this to SN 1998bw, which is thought to be related to GRB 980425. From this parameterization of the radio emission for SN 1998bw, we are able to describe the radio light curves for SN 1998bw in previously unattainable detail and show that a mildly relativistic blast wave interacting with a clumpy, structured CSM established by the wind from a massive progenitor provides a satisfactory description. Superimposed on a relatively constant mass loss of $\sim 2.6 \times 10^{-5}\ M_\odot\ \mathrm{yr}^{-1}$ are epochs of higher mass-loss rate, which increase the CSM density by a factor of $\sim 40\%$. At least two of these episodes can be identified and occur at an interval of ~ 9400 yr and a duration of ~ 3000 yr.

K. W. W. and M. J. M. wish to thank the Office of Naval Research (ONR) for the 6.1 funding supporting this research. Additional information and data on radio emission from SNe and GRBs can be found on http://rsd-www.nrl.navy.mil/7214/weiler/ and linked pages.

REFERENCES

Chevalier, R. A. 1982a, ApJ, 259, 302
———. 1982b, ApJ, 259, L85
———. 1998, ApJ, 499, 810
Chevalier, R. A., & Fransson, C. 1994, ApJ, 420, 268
Filippenko, A. 1998, IAU Circ. 6969
Filippenko, A., Matheson, T., & Barth, A. 1994, AJ, 108, 2220
Fishman, G. J., & Meegan, C. A. 1995, ARA&A, 33, 415
Fransson, C., & Björgsson, C.-I. 1998, ApJ, 509, 861
Gaensler, B. M., Manchester, R. N., Staveley-Smith, L., Tzioumis, A. K., Reynolds, J. E., & Kesteven, M. J. 1997, ApJ, 479, 845
Galama, T. J., et al. 1998a, IAU Circ. 6895
———. 1998b, Nature, 395, 670
———. 1999, A&AS, 138, 465
Goodman, J. 1986, ApJ, 308, L47
Immler, S., Aschenbach, B., & Wang, Q. D. 2001, ApJ, submitted
Iwamoto, K., et al. 1998, Nature, 395, 672

Jakobsen, P., et al. 1991, ApJ, 369, L63
Kay, L. E., Halpern, J. P., & Leighly, K. M. 1998, IAU Circ. 6969
Kellermann, K. I., & Pauliny-Toth, I. I. K. 1969, ApJ, 155, L71
Kulkarni, S. R., Bloom, J. S., Frail, D. A., Ekers, R., Wieringa, M., Wark, R., & Higdon, J. L. 1998a, IAU Circ. 6903
Kulkarni, S. R., et al. 1998b, Nature, 395, 663
Li, Z.-Y., & Chevalier, R. A. 1999, ApJ, 526, 716
Lidman, C., et al. 1998, IAU Circ. 6895
Lozinskaya, T. A. 1992, Supernovae and Stellar Wind in the Interstellar Medium (New York: AIP), 190
Manchester, R. N., et al. 2001, Publ. Astron. Soc. Australia, in press
Montes, M. J., Van Dyk, S. D., Weiler, K. W., Sramek, R. A., & Panagia, N. 1998, ApJ, 506, 874
Montes, M. J., Weiler, K. W., & Panagia, N. 1997, ApJ, 488, 792
Montes, M. J., Weiler, K. W., Van Dyk, S. D., Panagia, N., Lacey, C. K., Sramek, R. A., & Park, R. 2000, ApJ, 532, 1124
Natta, A., & Panagia, N. 1984, ApJ, 287, 228
Osterbrock, D. E. 1974, Astrophysics of Gaseous Nebulae (San Francisco: Freeman), 82
Paczynski, B. 1986, ApJ, 308, L43
Panagia, N., & Bono, G. 2001, in Proc. STScI Symp. (1999 May), The Largest Explosions since the Big Bang: Supernovae and Gamma Ray Bursts, ed. M. Livio, N. Panagia, & K. Sahu (Cambridge: Cambridge Univ. Press), 184
Patat, F., Cappellaro, E., Rizzi, L., Turatto, M., & Benetti, S. 1999, IAU Circ. 7215
Patat, F., & Piemonte, A. 1998, IAU Circ. 6918
Pian, E., et al. 1999, A&AS, 138, 463
———. 2000, ApJ, 536, 778
Readhead, A. C. S. 1994, ApJ, 426, 51
Sadler, E. M., Stathakis, R. A., Boyle, B. J., & Ekers, R. D. 1998, IAU Circ. 6901
Soffitta, P., et al. 1998, IAU Circ. 6884
Spyromilio, J. 1994, MNRAS, 266, L61
Sramek, R. A., Panagia, N., & Weiler, K. W. 1984, ApJ, 285, L59
Tinney, C., Stathakis, R., Cannon, R., & Galama, T. 1998, IAU Circ. 6896
Van Dyk, S. D., Sramek, R. A., Weiler, K. W., & Panagia, N. 1993a, ApJ, 409, 162
———. 1993b, ApJ, 419, L69
Van Dyk, S., Weiler, K., Sramek, R., Rupen, M., & Panagia, N. 1994, ApJ, 432, L115
Waxman, E., & Loeb, A. 1999, ApJ, 515, 721
Weiler, K. W., Panagia, N., & Sramek, R. A. 1990, ApJ, 364, 611
Weiler, K. W., Panagia, N., Sramek, R. A., van der Hulst, J. M., Roberts, M. S., & Nguyen, L. 1989, ApJ, 336, 421
Weiler, K. W., Panagia, N., Sramek, R. A., Van Dyk, S. D., Montes, M. J., & Lacey, C. K. 2001, in Proc. STScI Symp. (1999 May), The Largest Explosions since the Big Bang: Supernovae and Gamma Ray Bursts, ed. M. Livio, N. Panagia, & K. Sahu (Cambridge: Cambridge Univ. Press), 198
Weiler, K. W., Sramek, R. A., Panagia, N., van der Hulst, J. M., & Salvati, M. 1986, ApJ, 301, 790
Weiler, K. W., Van Dyk, S. D., Discenna, J. L., Panagia, N., & Sramek, R. A. 1991, ApJ, 380, 161
Weiler, K. W., Van Dyk, S. D., Panagia, N., & Sramek, R. A. 1992a, ApJ, 398, 248
Weiler, K. W., Van Dyk, S. D., Pringle, J., & Panagia, N. 1992b, ApJ, 399, 672
Williams, C. L., Panagia, N., Lacey, C. K., Weiler, K. W., Sramek, R. A., & Van Dyk, S. D. 2002, ApJ, submitted
Woosley, S. E., Eastman, R. G., & Schmidt, B. P. 1999, ApJ, 516, 788
Yin, Q. F. 1994, ApJ, 420, 152